Self-consistent Langmuir waves in resonantly driven thermal plasmas

R. R. Lindberg,[a] A. E. Charman, and J. S. Wurtele
Department of Physics, University of California, Berkeley, Berkeley, California 94720, USA
and Center for Beam Physics, Lawrence Berkeley National Laboratory, Berkeley, California 94720, USA

(Received 23 January 2007; accepted 3 October 2007; published online 6 December 2007)

The longitudinal dynamics of a resonantly driven Langmuir wave are analyzed in the limit that the growth of the electrostatic wave is slow compared to the bounce frequency. Using simple physical arguments, the nonlinear distribution function is shown to be nearly invariant in the canonical particle action, provided both a spatially uniform term and higher-order spatial harmonics are included along with the fundamental in the longitudinal electric field. Requirements of self-consistency with the electrostatic potential yield the basic properties of the nonlinear distribution function, including a frequency shift that agrees closely with driven, electrostatic particle simulations over a range of temperatures. This extends earlier work on nonlinear Langmuir waves by Morales and O'Neil [G. J. Morales and T. M. O'Neil, Phys. Rev. Lett. **28**, 417 (1972)] and Dewar [R. L. Dewar, Phys. Plasmas **15**, 712 (1972)], and could form the basis of a reduced kinetic treatment of plasma dynamics for accelerator applications or Raman backscatter. © *2007 American Institute of Physics*. [DOI: 10.1063/1.2801714]

I. INTRODUCTION

Much of the progress in understanding Langmuir waves has been restricted to the linear regime, wherein the perturbation of the plasma from its (Maxwellian) equilibrium is assumed "sufficiently small," such that second-order terms in the perturbation may be neglected. Under these conditions, one can derive the normal modes of the distribution function (the singular Case–Van Kampen modes[1,2]) or, alternatively, the Landau-damped "quasimodes" of the electric field.[3,4] A basic result of these linear analyses is that smooth, electrostatic perturbations tend to decay through the process of Landau damping.

That such damping is not universal was first pointed out by Bernstein, Greene, and Kruskal (BGK),[5] who included the plasma particles trapped in the electrostatic wave to formulate nonlinear distribution functions in one spatial dimension that give rise to time-independent electrostatic disturbances. Explicit constructions of sinusoidal, small-amplitude BGK waves were later derived by Holloway and Dorning,[6] in which they showed that arbitrarily small amplitude waves can exist without being Landau damped. BGK distributions are generally functions of the conserved electron energy $H=\frac{1}{2}m_e v^2-e\Phi(z)$ (where m_e is the electron mass, e is the magnitude of its charge, z is the longitudinal position, and v is the longitudinal velocity), whose charge perturbation self-consistently generates the electrostatic potential $\Phi(z)$ via Poisson's equation. Thus, BGK distributions are static solutions to the one-dimensional (1D) Vlasov-Poisson system (in Gaussian units),

$$\frac{d}{dt}f(v,z;t)=\frac{\partial f}{\partial t}+v\frac{\partial f}{\partial z}+e\frac{\partial \Phi}{\partial z}\frac{\partial f}{\partial v}=0, \tag{1a}$$

$$\frac{\partial^2}{\partial z^2}\Phi(z)=4\pi e\int dv f(v,z;t)-4\pi e n_i(z), \tag{1b}$$

where $f(z,v;t)$ is the electron distribution function at time t, and we consider the ions to have a time-independent background density $n_i(z)$.

In this paper, we introduce and characterize nonlinear Langmuir wave solutions to the 1D, nonrelativistic Vlasov-Poisson system Eq. (1) that are naturally occurring BGK-like waves. These waves (and the distribution functions that generate them) have particular relevance to laser-plasma physics, in that they arise dynamically as kinetic, nonlinear Langmuir waves in systems that are weakly driven on or near resonance. To obtain these solutions, we use canonical action-angle coordinates, finding that the bulk plasma is well-described by a simplified distribution function that is invariant in the canonical action. In this way, we obtain near-equilibrium solutions that approximate the fully time-dependent $f(v,z;t)$ when the resonant forcing is small. These invariant-in-action distributions are similar to the adiabatic theory originally proposed by Dewar[7] and recently expanded upon by Bénisti and Gremillet,[8] although we show that it is a different action that is conserved in the general problem. While this distinction is relatively unimportant for waves whose potential energy is less than the thermal energy as considered in Ref. 8, it is of marked significance for larger amplitude waves or colder plasmas.

Because these nonlinear, kinetic Langmuir waves arise naturally in slowly driven systems, their bulk properties can be used to illuminate basic plasma processes and to obtain reduced descriptions of complex phenomena. For example, the nonlinear frequency shift of the thermal Langmuir resonance is an important quantity in any reduced model of Raman scattering in plasma,[9–11] and our results extend those of Morales and O'Neil[12] and Dewar[7] to colder plasmas and to larger electrostatic potentials $\Phi(z)$. We leave the numerical

[a]Electronic mail: rlindberg@berkeley.edu.

implementation of such Langmuir envelope models in a three-wave-type code to future work.

We introduce the nonlinear distribution function in Sec. II. We begin with the single-particle equations of motion for a weakly driven system, and proceed to introduce the relevant action-angle coordinates. Assuming that the electrostatic amplitudes vary slowly on the particle bounce time, we use the results of Refs. 13–15 to show that the electron distribution function remains approximately invariant in the action even for those particles that cross the separatrix; we also augment this discussion with a geometric argument leading to these results in terms of phase-space area conservation. Next, in Sec. III, we use Coulomb's law and the demands of self-consistency to derive the functional relationship between the mean area and the amplitude of the potential. This fully specifies the distribution, from which we then extract the natural frequency of the nonlinear BGK-type wave. To compare this theory with previous results, we present the small-amplitude limits in Sec. IV, for which the dynamics can be approximated by that of a physical pendulum. Finally, we compare the frequency of these nonlinear Langmuir waves to those obtained from self-consistent particle simulations in Sec. V for thermal plasmas with $0.2 \leq k\lambda_D \leq 0.4$, where $\lambda_D \equiv v_{\mathrm{th}}/\omega_p$ is the electron Debye length and k is the Langmuir wavenumber. Some concluding remarks and possible applications are given in Sec. VI.

II. THE NONLINEAR DISTRIBUTION FUNCTION IN A WEAKLY DRIVEN PLASMA

In this section, we present the single-particle dynamical equations relevant to a weakly driven plasma wave in the action-angle formalism. This results in a natural separation of time scales, from which a simplified approximate form of the nonlinear electron distribution function can be determined.

A. Single-particle equations

In what follows, we ignore transverse variation, assuming that the dominant dynamics occur along the longitudinal (z) axis. We also neglect any motion of the background ions, and furthermore assume that the longitudinal force on the electrons can be divided into two components: the first is given in terms of an external driving potential $V(z,t)$, which could arise, for example, from a ponderomotive force derived from the beating between two lasers. The second is given by the self-consistent electrostatic field $E_z(z,t)$ of the plasma electrons. Thus, Newton's equation of motion for a longitudinal coordinate $z(t)$ of any electron is given by

$$\frac{d^2}{dt^2}z(t) = -\frac{e}{m_e}E_z(z,t) - \frac{1}{m_e}\frac{\partial}{\partial z}V(z,t). \tag{2}$$

The restriction to 1D, Newtonian dynamics should be valid provided that the transverse "spot size" of the external exciting potential is large compared to the collisionless skin depth c/ω_p of the electron plasma, and that both the forcing is sufficiently weak and the temperature sufficiently low so that all components of the electron velocity remain much smaller than c in magnitude.

We furthermore assume that the external drive may be characterized in terms of a dimensionless amplitude $\mathcal{V}(z,t)$ modulating a carrier oscillation at frequency ω and wavenumber k,

$$\frac{k^2}{m_e\omega_p^2}V(z,t) = \mathcal{V}(z,t)\sin(\omega t + kz), \tag{3}$$

where $\omega_p \equiv (4\pi n_0 e^2/m_e)^{1/2}$ is the cold, linear plasma frequency corresponding to the (uniform) equilibrium electron density n_0, and the dimensionless amplitude $\mathcal{V}(z,t)$ varies slowly on the spatio-temporal scales set by the carrier phase,

$$\left|\frac{\partial}{\partial t}\ln\mathcal{V}(z,t)\right| \ll \omega, \quad \left|\frac{\partial}{\partial z}\ln\mathcal{V}(z,t)\right| \ll k. \tag{4}$$

The nearly periodic, weak external drive then sets a natural spatial length scale for the slowly evolving, self-consistent electrostatic field $E_z(z,t)$.

To help motivate our subsequent choices of coordinates and separation of time scales, we express the electric field in the following manner:

$$E_z \equiv E_0 - \frac{\partial\Phi}{\partial z} = \frac{m_e\omega_p^2}{ek}\left[\mathcal{E}_0(z,t) - \frac{1}{k}\frac{\partial}{\partial z}\phi(z,t)\right]. \tag{5}$$

In Eq. (5), the dimensionless field $\mathcal{E}_0 \equiv (ek/m_e\omega_p^2)E_0$ represents the component of the electric field that varies over spatial lengths significantly longer than $1/k$ (and so may be taken as an effectively z-independent "DC" field over any one given wavelength, or "bucket"), while the dimensionless potential $\phi(z,t)$ encapsulates the fundamental and higher harmonics of the resonantly excited Langmuir wave. Thus, we expand $\phi(z,t)$ as a Fourier series of dimensionless eikonal amplitudes,

$$\phi(z,t) = \sum_{n=1}^{\infty}\phi_n(z,t)\cos\{n[(\omega t + kz) + \xi(z,t)]\}. \tag{6}$$

In the limit of small forcing, we now express Eq. (2) as a Hamiltonian system appropriate for action-angle variables by introducing the dimensionless time $\tau \equiv \omega_p t$, the scaled (linear) frequency $\omega_L \equiv \omega/\omega_p$, and the dimensionless phase-space coordinates given by the phase θ in the electrostatic wave and its corresponding canonical momentum p,

$$\theta \equiv \omega t + kz + \xi(\tau), \tag{7a}$$

$$p \equiv \dot{\theta} - \dot{\xi} - a_z \equiv k\dot{z} + \omega_L + \int_{-\infty}^{\tau} d\tau'\,\mathcal{E}_0(\tau'), \tag{7b}$$

where $\xi(\tau)$ and $\mathcal{E}_0(\tau)$ are the single-particle analogs of the phase shift and DC component of the electric field introduced above, for any chosen wavelength (or "bucket") of interest, and where we have defined $a_z(\tau) \equiv -\int d\tau'\,\mathcal{E}_0(\tau')$ in terms of the integrated DC component of the scaled electric field $\mathcal{E}_0(\tau)$. The overdot in Eq. (7b) denotes the normalized time derivative $d/d\tau \equiv (1/\omega_p)d/dt$. We next define the frequency shift $\delta\omega \equiv \dot{\xi}$ and neglect the *direct* effects of the external drive on the trajectory of any individual electron in comparison to the effects of the induced space-charge field, under the assumption that $\mathcal{V} \ll \max|\phi| \equiv \phi_{\max}$, so that the

second-order equation of motion Eq. (2) can be replaced with the first-order pair

$$\dot{\theta} = p + \delta\omega(\tau) + a_z(\tau), \quad \dot{p} = \frac{\partial}{\partial\theta}\phi(\theta,\tau), \tag{8}$$

where $\phi(\theta,\tau)$ is taken as periodic over the single bucket of interest at fixed time τ, again consistent with our eikonal assumptions Eq. (4).

The system Eq. (8) can be obtained from the Hamiltonian

$$\mathcal{H}(p,\theta;\tau) = \tfrac{1}{2}[p + \delta\omega(\tau) + a_z(\tau)]^2 - \phi(\theta,\tau), \tag{9}$$

from which we see that $\delta\omega(\tau)$ emerges as a consequence of considering the motion in the wave frame moving with the *instantaneous* Langmuir phase velocity, and that, as our notation has anticipated, the time-integrated field $a_z(\tau)$ can be interpreted as the $\hat{z}$ component of the scaled vector potential, so that its presence in Eq. (9) appears completely natural when we realize that p is a *canonical* momentum conjugate to the phase θ, rather than the *kinetic* momentum. Note that in one-dimensional, *periodic* geometry, the chosen Coulomb gauge condition

$$\boldsymbol{\nabla}\cdot\boldsymbol{A} = \frac{\partial}{\partial z}A_z(z,t) = 0$$

still admits the possibility of a *geometrically* longitudinal component $A_z(t)$ that is spatially uniform but possibly time-dependent. It is precisely this component that previous authors have neglected, resulting in a different definition of "the action." In Ref. 16, Dewar did include the DC electric field when considering the effects of trapped electrons on ion-acoustic waves, and in that context obtained an action identical to our Eq. (10). Our results reveal that as the wave energy becomes larger than that associated with the thermal motion, the contributions of both the DC field as encapsulated in $a_z(\tau)$ and the contributions of the higher-order harmonics represented in $\phi(\theta,\tau)$ must be included in order to obtain a canonical action that can be adiabatically conserved in the presence of a nonlinear Langmuir wave frequency which, as is well known, remains independent of wave amplitude in the limit of vanishing thermal and relativistic effects.

Now, we summarize a few general features regarding the Hamiltonian Eq. (9). The frozen orbits are defined as the level sets $\mathcal{H}(p,\theta;\tau)=H$ at a fixed time τ, for which the parameters ϕ_n, $\delta\omega$, and a_z are constant and the motion is periodic. A representative phase portrait of the frozen orbits is in Fig. 1, superposed on a numerical phase-space snapshot taken from a self-consistent particle simulation. Generically, we see that phase space is divided into three distinct regions, separated by the trajectories joining the hyperbolic fixed points at $\theta=\pm\pi, p=-\delta\omega-a_z$, for which $H=\phi_{\max}$. These separatrices partition the "rotational" motion in regions I and III, for which $H>\phi_{\max}$, from the "libration" about the stable fixed point at $\theta=0$ in region II, where $H<\phi_{\max}$. Associated with these frozen orbits, there exists a canonical transformation to action-angle coordinates $(p,\theta;\tau)\leftrightarrow(J_c,\Psi;\tau)$, with

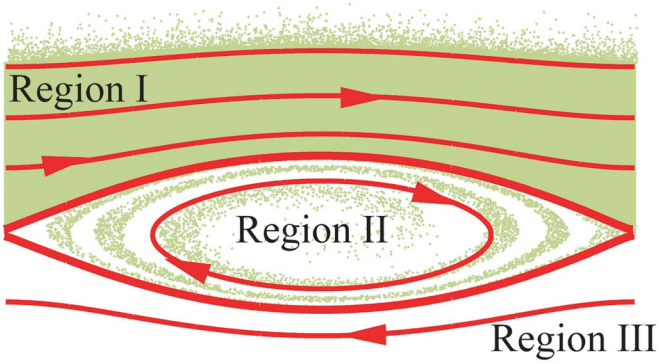

FIG. 1. (Color online) Phase-space schematic for frozen orbits in the presence of a monochromatic wave overlaid on the results of a self-consistent particle simulation. Region I (above the separatrices) consists of the plasma bulk making up the wave; region II contains the trapped particles between the separatrices; region III contains those particles moving too fast to be trapped in the wave.

the (complete) *canonical* action proportional to the phase-space area of the frozen orbit,

$$J_c(H;\tau) \equiv \frac{1}{2\pi}\oint d\theta p(\theta,H;\tau)$$
$$= \frac{1}{2\pi}\oint d\theta\left\{\sqrt{2[H+\phi(\theta;\tau)]} - \delta\omega(\tau) - a_z(\tau)\right\}. \tag{10}$$

The integration in Eq. (10) proceeds about the frozen orbit of energy H, which is intrinsically closed for the trapped orbits, and will be topologically closed for the untrapped orbits. For these untrapped orbits, the branch of the square root is chosen according to the sign of the momentum p in the moving frame, so that J_c is negative for particles moving faster than the wave phase velocity. Note that this action J_c differs through the appearance of $a_z(\tau)$ from the action J_{BG} which Bénisti and Gremillet[8] assume is an adiabatic invariant, which in our notation becomes

$$J_{BG} \equiv \frac{1}{2\pi}\oint d\theta\{\sqrt{2[H+\phi(H;\tau)]} - \delta\omega(\tau)\}, \tag{11}$$

and also differs by the inclusion of both the DC component and higher-order potential terms from the "physical pendulum" action J_p used by Dewar,[7] who neglected a_z and further assumed $\phi=\phi_1(\tau)\cos\theta$.

The utility of our action-angle coordinates in this setting lies in their division of the motion into two distinct time scales: the natural frequency of the canonical angle $\dot{\Psi}\sim 1$ gives the time over which particles complete oscillations in the wave, during which time the action varies (nonsecularly) by a small amount proportional to the external drive, $\dot{J}_c\sim\mathcal{V}$. Furthermore, since J_c is related geometrically to the phase-space area, incompressible Hamiltonian flow significantly constrains its evolution, such that it is in fact an adiabatic invariant of the motion over a range of wave amplitudes, unlike either J_{BG} or J_p in general. We use these facts in the next section to obtain an approximate, simplified description of the nonlinear electron distribution function.

B. The invariant-in-action distribution function

The central assumption for our subsequent discussion is that the Langmuir wave amplitude and frequency are slowly evolving, meaning that the parameters $\phi_n(\tau)$, $\mathcal{E}_0(\tau)$, and $\delta\omega(\tau)$ of the Hamiltonian do not vary appreciably over one period of the motion. For those particles trapped deeply in region II, the frequency of motion is of the order of the bounce frequency $\sim\sqrt{\phi_1}$, so that for nearly all the particles, i.e., all except the exponentially few in a narrow range about the separatrix, the condition of "slowness" can be written as

$$\frac{1}{\sqrt{\phi_1}}\left|\frac{d}{d\tau}\ln\phi_1\right| \sim \frac{1}{\sqrt{\phi_1}}\left|\frac{d}{d\tau}\ln\delta\omega\right| \sim \frac{1}{\sqrt{\phi_1}}\left|\frac{\mathcal{E}_0(\tau)}{a_z(\tau)}\right| \sim \epsilon \ll 1. \tag{12}$$

Under the conditions (12), it follows that the action is an adiabatic invariant for electrons deep in regions I, II, or III, meaning that J_c is conserved [to an extent depending on the degree of smoothness of the drive $\mathcal{V}(\tau)$] for times of order $1/\epsilon \sim 1/\mathcal{V}$. This holds provided that the frozen frequency associated with the motion does not vanish.

However, as particles approach the separatrix, where $H \to \phi_{\max}$ and the nonlinear frequency vanishes logarithmically, traditional adiabatic theory is inapplicable. In this case, Best[18] first reported numerical evidence that a modified adiabatic theory may yet apply. Rigorous theoretical results were later obtained by three independent groups (Cary, Escande, and Tennyson,[13] Neishtadt,[14] and Hannay,[15] generalizing early work by Timofeev[17]) by asymptotically matching the standard solutions of adiabatic motion to those appropriate near the separatrix. The essential finding of these authors is that only an exponentially small fraction of initial conditions pass sufficiently close to the hyperbolic fixed point to significantly modify their orbits, so that the vast majority of the particles experience, to lowest order, just a modification of their canonical action reflecting the discontinuous change in orbit topology.

In our symmetric Hamiltonian (meaning that particles in region I and III see the same potential), this just corresponds to a doubling of the action as the motion transitions from untrapped or "rotational" to trapped or "librational" motion. For a particle with initial action $J_c(\tau=0)$ in either region I or III, the final action $J_c(\tau)$ after crossing into II is given by $J_c(\tau)=2|J_c(0)|+O(\epsilon)$. Thus, we see that the distribution remains essentially invariant in the action even for those particles that approach and cross the separatrix (accounting, of course, for the geometric factor of ±2 when trapped). Furthermore, it is easy to see that far from the separatrix the canonical angle Ψ evolves essentially according to the unperturbed motion, so that the distribution initially uniform in Ψ remains so under the slowly evolving Hamiltonian $\mathcal{H}(p,\theta;\tau)$. Thus, assuming that the conditions (9) are satisfied, the distribution far from the separatrices is constant in the Ψ-J_c plane [to within $O(\epsilon)$].

While we have seen that the action is essentially conserved upon crossing the separatrix, we need to determine how the angle evolves to obtain the full distribution function. In this case, we invoke the results of phase evolution by Cary and Skodje[19,20] and Elskens and Escande,[21] obtained by analyzing the near-separatrix motion in slowly evolving systems. For the majority of the particles, the canonical angle is mapped smoothly through the separatrix. In a naive picture, the infinitesimal strip of particles in region I with action J_c and spread over $0 \le \Psi < 2\pi$ is mapped across the separatrix to the strip from $0 \le \Psi < \pi$ that subsequently rotates in region II. As shown in Refs. 19–21, this picture is essentially accurate up to corrections of $O(\epsilon)$, excluding the exponentially small [specifically, $O(e^{-1/\epsilon}/\epsilon)$] fraction of particles that pass very close to the hyperbolic fixed point. Since these particles can spend an arbitrarily long time tracing the stable manifold, they lead to long, diffuse phase-space tendrils. Neglecting these few but pathological particles, to each initial action is associated a strip of particles that is mapped to one-half the canonical angle range upon crossing the separatrix. As the wave grows, this proceeds for each successive action strip, with each one displaced from the next by some relative phase shift in the canonical angle. The relative phase between increasing action strips increases up to 2π, for which the action will have increased by $O(\epsilon)$ (see Ref. 21 for a detailed discussion). In this way, we argue that the distribution remains uniform in Ψ to within $O(\epsilon)$ even when crossing the separatrix, provided only that the slowness conditions (12) are met.

Hence, the distribution essentially remains constant in the Ψ-J_c plane, except that as particles are trapped their actions are mapped to twice their initial values. While this picture is not precisely correct for all times (as we will see, a uniform in Ψ, i.e., phase-mixed, distribution can experience no Landau damping), it does encapsulate the long-time dynamics, for which particles with different nonlinear frequencies phase-mix. Note that although this requires a coarse-graining of the distribution, O'Neil showed that the phase-space area over which such coarse-graining is required vanishes as time progresses.[22] In the next section, we will describe a geometric argument for action conservation across slowly evolving separatrices that also illuminates how the complicated evolution in Ψ and J_c during trapping nevertheless results in a nearly invariant distribution function $f(J_c,\Psi;\tau)$ except for topological effects upon crossing.

C. A geometric picture of the invariant-in-action distribution: The Poincaré-Cartan integral invariant

As indicated in the preceding section, the change in J_c upon crossing a slowly evolving separatrix is approximately given by an overall multiplicative factor corresponding to the change in orbit topology. For a geometric argument of this result, we first review the Poincaré-Cartan integral invariant in the context of a one-degree-of-freedom nonautonomous system. Suppose that two (piecewise smooth, equivalently oriented, closed) curves γ_1 and γ_2 encircle the same tube of trajectories generated by $\mathcal{H}(\theta,p;\tau)$ in the extended (2+1)-dimensional space $[(\theta,p;\tau)]$. In this case, the integrals of the 1-form $p\,d\theta - \mathcal{H}dt$ along the two curves are equal.[23] If we consider both γ_1 and γ_2 to consist of simultaneous phase-space points (i.e., each lies in a plane of constant τ), we have

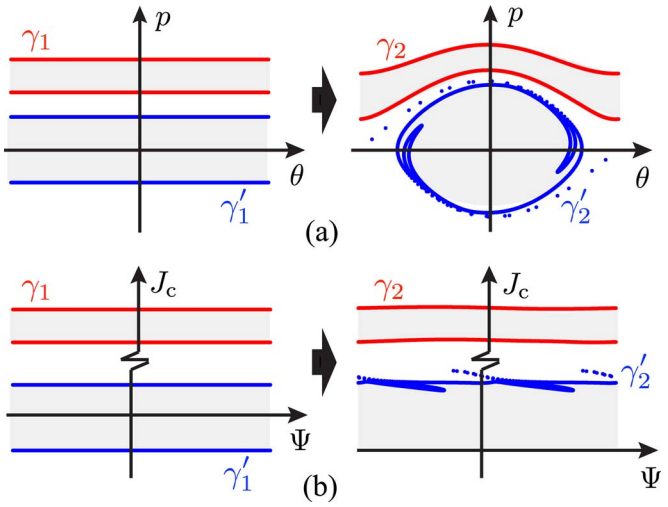

FIG. 2. (Color online) Dynamics of two different tubes of trajectories slowly driven on resonance. The particles remain essentially uniform in Ψ and can be identified [to $O(\epsilon)$] with frozen orbits of action along the upper and lower portions of γ. Since the area enclosed by γ_1 equals that enclosed by γ_2, the relative J_c is invariant. This holds to $O(\epsilon)$ even for the trapped particles along γ'. Choosing a family of curves γ_1 indicates that the distribution is essentially invariant in J_c.

$$\oint_{\gamma_1} d\theta p = \oint_{\gamma_2} d\theta p, \tag{13}$$

which is a form of Liouville's theorem, where the "final" curve $\gamma_2=\gamma_1(\tau)$ can be interpreted as the image of the "initial" curve γ_1 under the flow. These integrals should not be confused with the action J_c: while J_c is evaluated along the frozen orbit associated with a given point in phase space, the curves $\gamma_{1,2}$ in Eq. (13) are determined by a family of trajectories evolving under the flow of $\mathcal{H}$. Nevertheless, under slow evolution given by Eq. (12), we will argue that the curves $\gamma_{1,2}$ can be associated, to within $O(\epsilon)$, with appropriate pairs of these frozen orbits, so that in this case Eq. (13) indicates that the relative change in J_c among the particles is small.

First we consider those electrons that begin and remain far from the separatrices. Specifically, we consider an initial curve γ_1 defined by the locus of points initially at two values of velocity (or action) as shown with the upper (red) curves of Figs. 2(a) and 2(b). Under Hamiltonian flow, Eq. (13) dictates that the phase-space area (in either the θ-p or Ψ-J_c plane) enclosed by γ_1 equals that bounded by γ_2, so that the top shaded areas are identical in both Figs. 2(a) and 2(b). While this is true in general, it is stronger if approximate conclusions can be drawn when the parameters of $\mathcal{H}$ vary slowly in time.

Far from the separatrices, the set of particles vary in action J_c by an amount of $O(\epsilon)$ during an orbit, while remaining essentially uniform in angle Ψ. Thus, the evolved curve γ_2 can be identified [to within $O(\epsilon)$] as the conjunction of two frozen orbits with definite actions, implying that the initial phase-space rectangle remains essentially a rectangle in the Ψ-J_c plane. This is evidenced in Fig. 2(b), which shows that the evolved curve γ_2 is described, neglecting the $O(\epsilon)$ undulations, by two nearly straight lines in J_c. Note that this result differs dramatically from the deformation of γ_1 apparent in the θ-p plane in Fig. 2(a). By considering a foliation of nested flux tubes encircled by $\gamma_{1,2}$ of various actions, we can see that slow evolution leads to an *untrapped* particle distribution that is invariant in the action deviation $J_c-\bar{J}_c$, with only a possible slow temporal change in the mean action $\bar{J}_c=\bar{J}_c(\tau)$ of the untrapped particles. Assuming that the appropriate canonical action is used, which includes the frequency shift $\delta\omega$ and the time-integrated DC component $a_z(\tau)$, standard adiabatic theory implies that this action is conserved, so that $\bar{J}_c(\tau)=0$ for the untrapped distribution (and, as we will confirm momentarily, for the trapped and therefore overall distributions as well). In contrast, instead using J_{BG} which implicitly assumes that $\mathcal{E}_0(\tau)\equiv 0$ would result in an apparent shift in the action by $\bar{J}_{BG}(\tau)=a_z(\tau)\neq 0$.

Neglecting the exponentially few particles that closely approach the hyperbolic fixed point, we know that the action still only changes by $O(\epsilon)$ during any oscillation, while the particles remain essentially uniform in Ψ. Thus, we can again associate with the evolved curve γ_2' a frozen orbit of definite action [up to $O(\epsilon)$ corrections], so that similar conclusions obtained for particles far from the separatrices apply even to those that cross the separatrix. This is indicated in the lower areas of Fig. 2, where we consider the (blue) curve γ_1' that is initially symmetric about the phase velocity, for which the Poincaré-Cartan invariant is proportional to twice the action of the upper boundary. In Fig. 2(b), we see that γ_1' is mapped to γ_2' across all of Ψ and to which can (approximately) be ascribed an action that is twice that of the upper boundary of γ_1'. Since γ_2' now lies [to within $O(\epsilon)$] along the trapped frozen orbit, the Poincaré-Cartan invariant Eq. (13) leads to canonical action conservation for the trapped particles, and we may infer that the phase-mixed distribution for the *trapped* particles will remain approximately invariant in J_c itself. Since the average action of the trapped particles should approximately vanish, $J_c=J_{BG}$ for these trapped particles, but not for the untrapped bulk.

To illustrate these invariant-in-action distributions, we have performed a number of single-wavelength particle simulations, described further in Sec. V, that solve the periodic Vlasov-Poisson system. We include representative results in Fig. 3, obtained with a drive potential $\mathcal{V}=0.01$ and an initially Maxwellian velocity distribution whose width corresponds to $k\lambda_D\equiv\sigma=0.3$. In Fig. 3(a), we observe the characteristic flattening of $f(v)$ near the phase velocity that is associated with particle trapping. For the same values of ϕ_1, Fig. 3(b) demonstrates that the distribution in J_c (integrated over Ψ) remains nearly Gaussian in action [but note that we divided J_c by 2 in the resonance region to make $f(J_c)$ smooth across the upper separatrix, and that the passing particles are too few to make the plot]. Furthermore, except for slight oscillations in the resonance region, $f(J_c)$ has a constant variance σ^2 and a constant mean at ω_L.

III. NONLINEAR SELF-CONSISTENCY: PARAMETRIZING THE DISTRIBUTION

In the preceding section, we showed that the distribution function approximately satisfies our action ansatz, remaining

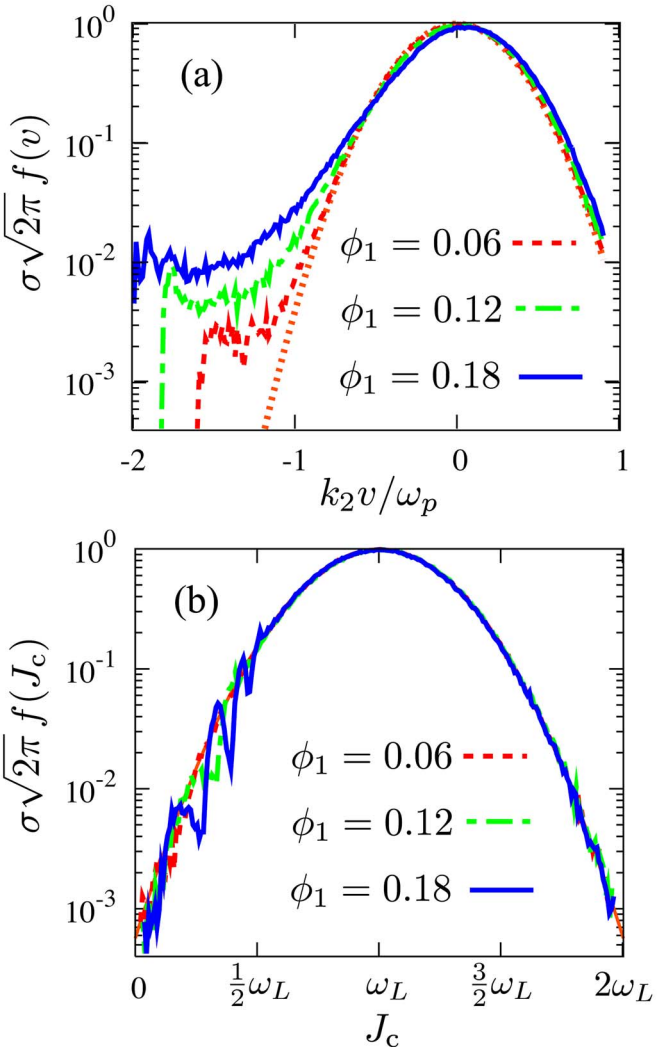

FIG. 3. (Color online) Wavelength-averaged distribution function for three values of the electrostatic potential ϕ_1 using $k\lambda_D=0.3$. In velocity space, (a) shows the flattening of $f(v)$ about the phase velocity $kv/\omega_p \approx 1.16$ characteristic of particle trapping (the initial Maxwellian is included for reference). Meanwhile, (b) demonstrates that the distribution remains nearly invariant in the action, with slight oscillations of $f(J_c)$ in the resonance region (note that we divided J_c by 2 for the trapped particles to make it continuous).

essentially invariant in the canonical action J_c of Eq. (10), apart from a multiplicative jump reflecting the change in frozen orbit topologies upon crossing the separatrix. Now we turn to parametrizing such distributions by imposing the constraints of self-consistency, namely, that the assumed $f(J_c)$ must also act as a source for the appropriate electric field via Maxwell's equations. Because J_c is defined only in terms of the sum $\delta\omega+a_z$, Poisson's equation is insufficient to determine $\delta\omega$; this indeterminacy is alleviated by applying the Ampère-Maxwell law, as was first noted in Ref. 16.

To facilitate our subsequent discussion (and defer direct reference to $\mathcal{E}_0$), we introduce another phase-space area $\mathcal{I}$ related to the action J_c in the following manner:

$$\mathcal{I}(H;\tau) = \begin{cases} J_c(H;\tau) + \delta\omega(\tau) + a_z(\tau) & \text{if } H \geq \phi_{\max} \\ \dfrac{1}{2} J_c(H;\tau) & \text{if } H < \phi_{\max} \end{cases}. \quad (14)$$

We define $\mathcal{I}$ primarily for mathematical convenience, but note that the form of the distribution function with respect to $\mathcal{I}$ is simpler than that for J_c itself. In particular, for a slowly driven plasma whose distribution function is initially uniform in space and Maxwellian in momentum, adiabatic evolution of J_c guarantees that the distribution function remains essentially Gaussian in $\mathcal{I}$, as indicated explicitly in Eq. (24) below.

In the next subsection, we obtain an expression for the mean $\bar{\mathcal{I}}(\tau)$. Having parametrized $f(J_c)$, we use this to determine the frequency shift $\delta\omega$ of the wave, which we subsequently compare to the frequency determined numerically from a self-consistent particle simulation.

A. Self-consistency and the Poisson equation

First, our nonlinear distribution function must give rise to a charge separation commensurate with the electrostatic potential $\phi(z,t)$. This is summarized by the Poisson equation (1b), which, in dimensionless form, is

$$\frac{\partial^2 \phi}{\partial \zeta^2} = \frac{1}{n_0} \int dv f[\mathcal{I}(v,\zeta;\phi),\bar{\mathcal{I}}(\tau)] - 1, \quad (15)$$

where $\zeta \equiv kz$ is employed as a scaled longitudinal coordinate. The Poisson equation (15) constitutes an implicit relationship for the average area $\bar{\mathcal{I}}$ in terms of the full potential ϕ; in order to solve this numerically, we use the dimensionless Fourier expansion Eq. (6). Multiplying Eq. (15) by $\cos\theta$ and integrating over a wavelength, we obtain

$$0 = \left(1 + \frac{2}{\phi_1}\langle \cos\theta \rangle\right)\phi_1 \equiv \varepsilon(\bar{\mathcal{I}};\phi)\phi_1, \quad (16)$$

where we have introduced the "nonlinear dielectric function" $\varepsilon(\bar{\mathcal{I}};\phi)$, and define the phase-space average $\langle\cdot\rangle$ via

$$\langle \mathcal{X} \rangle \equiv \frac{1}{n_0}\int_{-\infty}^{\infty} dv \frac{1}{2\pi}\int_{-\pi}^{\pi} d\zeta f(\mathcal{I}(v,\zeta;\phi),\bar{\mathcal{I}}(\tau))\mathcal{X}(v,\zeta).$$

Furthermore, the higher harmonics of the potential are given similarly by

$$\phi_n = -\frac{2}{n^2}\langle \cos(n\theta) \rangle. \quad (17)$$

We consider Eqs. (16) and (17) to be implicit expressions for $\bar{\mathcal{I}}$ and the harmonics ϕ_n in terms of the fundamental ϕ_1. Our procedure for numerically solving these equations can be summarized by the following (presumably convergent) series:

$$\bar{\mathcal{I}}^{j+1} = \bar{\mathcal{I}}^j - \frac{\varepsilon(\bar{\mathcal{I}}^j;\phi^j)}{\dfrac{\partial}{\partial \bar{\mathcal{I}}^j}\varepsilon(\bar{\mathcal{I}}^j;\phi^j)}, \quad (18a)$$

$$\phi_n^{j+1} = -\frac{2}{n^2}\langle \cos(n\theta) \rangle. \quad (18b)$$

To solve Eq. (18), we choose a level for ϕ_1 near zero and calculate the mean area $\bar{\mathcal{I}}^1$ and harmonics ϕ_n^1, assuming initial values $\bar{\mathcal{I}}^0=\omega_L$ and $\phi_n^0=0$ [the expression for ω_L is subsequently given by Eq. (31)]. We then iterate Eq. (18) until

$\varepsilon(\bar{\mathcal{I}},\phi)\approx 0$, for which we have $\bar{\mathcal{I}}(\phi_1)$ and the exact potential $\phi(\zeta)$. We then use these as initial values for the next iteration at a larger value of ϕ_1, thereby obtaining the entire function $\bar{\mathcal{I}}(\phi_1)$.

B. The Ampère-Maxwell law and resulting frequency shift

To complete the characterization of the action distribution function, we calculate an expression for the frequency shift as a function of ϕ_1 and the mean $\bar{\mathcal{I}}$. To determine $\delta\omega$, we use the fact that the plasma tends to establish a return current that balances any long-range electric fields. In this case, the longitudinal component of the Ampère-Maxwell equation, including the contribution from the $\hat{z}$ component of the Coulomb-gauge vector potential, is given by

$$\frac{\partial}{\partial\tau}\left(\mathcal{E}_0(\zeta,\tau)+\frac{\partial\phi}{\partial\zeta}\right)=\frac{1}{n_0}\int dv f[\mathcal{I}(v,\zeta;\phi),\bar{\mathcal{I}}(\tau)]\frac{kv}{\omega_p}.$$

Integrating over one period in ζ, we have

$$\frac{\partial}{\partial\tau}\left(\mathcal{E}_0-\frac{\phi(\pi,\tau)-\phi(-\pi,\tau)}{2\pi}\right)=\left\langle\frac{kv}{\omega_p}\right\rangle, \tag{19}$$

where we have now allowed for slight violations of our periodic boundary conditions consistent with our eikonal assumptions, but since we assume the electrostatic field $\mathcal{E}_0(\zeta,\tau)$ and potential $\phi(\zeta,\tau)$ are slowly varying, and the latter must be almost periodic, the expression Eq. (19) must approximately vanish. Note that this is exact in the limit of a time-independent, nonlinear mode (similar to the BGK case), and expresses the fact that in 1D geometry with immobile (i.e., effectively infinitely massive) ions, the plasma electrons in a Langmuir wave carry no net momentum.[24] Using

$$v\propto\left(\frac{d}{d\tau}\theta-\delta\omega-\omega_L\right),$$

we have

$$\delta\omega(\tau)=\left\langle\frac{d}{d\tau}\theta\right\rangle-\omega_L. \tag{20}$$

We again note, as shown in Ref. 25, that the scale length for the transverse variation must be much greater than the collisionless skin depth c/ω_p for the one-dimensional approximation associated with Eq. (20) to hold.

To summarize, our model consists of assuming that the distribution function is adiabatically invariant in the action J_c given in Eq. (10). To parametrize the distribution, we calculate the average area $\bar{\mathcal{I}}$ [defined in terms of J_c in Eq. (14)] as a function of ϕ_1 by iteratively solving Eq. (18), where the nonlinear dielectric $\varepsilon(\bar{\mathcal{I}},\phi_1)$ is given by Eq. (16). We then use the (invariant) distribution $f[\mathcal{I};\bar{\mathcal{I}}(\phi_1)]$ to obtain the frequency shift via the phase-space average Eq. (20); we relate $d\theta/d\tau$ to $\mathcal{I}$ via the Hamiltonian Eq. (9).

IV. CONNECTIONS TO PREVIOUS WORK

To make connections with previously published results, we compute the linear and small-amplitude limits of the mean area $\bar{\mathcal{I}}$ and frequency shift $\delta\omega$. In this limit, for which the electrostatic potential energy is much greater than the thermal energy, i.e., $\phi_1\ll\sigma^2\equiv k^2\lambda_D^2$, we can assume that the scalar potential consists of a single harmonic, so that $\phi_n\approx 0$ for $n\geq 2$ and $\mathcal{E}_0\approx 0$. This implies that the Hamiltonian Eq. (9) becomes that of a classical physical pendulum,

$$\mathcal{H}(p,\theta;\tau)\rightarrow\tfrac{1}{2}[p+\delta\omega(\tau)]^2+\phi_1(\tau)(1-\cos\theta). \tag{21}$$

In this case, we can obtain analytical results suitable for direct comparison to those previously published.

A. The pendulum Hamiltonian relevant for small ϕ

In this subsection, we review the well-known dynamics of the pendulum Hamiltonian Eq. (21) relevant for calculating the frequency shift in the small-amplitude limit. The phase-space area $\mathcal{I}$ of the pendulum can be calculated analytically (see, e.g., Ref. 26), resulting in

$$\mathcal{I}(\kappa)=\begin{cases}\mathcal{I}_s\kappa\mathcal{E}(1/\kappa) & \text{if } |\kappa|\geq 1\\ \mathcal{I}_s[\mathcal{E}(\kappa)+(\kappa^2-1)\mathcal{K}(\kappa)] & \text{if } |\kappa|<1\end{cases}, \tag{22}$$

where $\kappa^2\equiv H/2\phi_1$ is the scaled energy, $\mathcal{I}_s\equiv 4\sqrt{\phi_1}/\pi$ is the action of the upper separatrix, and the complete elliptic integrals of the first and second kind, respectively, are defined via

$$\mathcal{K}(\kappa)\equiv\int_0^{\pi/2}\frac{d\alpha}{\sqrt{1-\kappa^2\sin^2\alpha}},$$

$$\mathcal{E}(\kappa)\equiv\int_0^{\pi/2}d\alpha\sqrt{1-\kappa^2\sin^2\alpha}.$$

Furthermore, the nonlinear period of the pendulum is

$$\mathcal{T}(\kappa)=\begin{cases}\dfrac{2}{\kappa\sqrt{\phi_1}}\mathcal{K}(1/\kappa) & \text{if } |\kappa|\geq 1\\ \dfrac{4}{\sqrt{\phi_1}}\mathcal{K}(\kappa) & \text{if } |\kappa|<1.\end{cases} \tag{23}$$

Using the definitions Eq. (22), the invariant distribution function naturally divides into four pieces: one of untrapped particles in region I, another for untrapped particles below both separatrices in region III, and two associated with the trapped particles of region II, depending on whether they enter from region III or region I; these are, respectively, encapsulated in the following definitions:

$$f_{\mathrm{I}}(\kappa;\tau)\equiv\frac{\mathcal{I}_s\mathcal{K}(1/\kappa)}{\sigma\sqrt{2\pi}}\exp\left\{-\frac{1}{2\sigma^2}[\mathcal{I}(\kappa)-\bar{\mathcal{I}}]^2\right\}, \tag{24a}$$

$$f_{\mathrm{III}}(\kappa;\tau)\equiv\frac{\mathcal{I}_s\mathcal{K}(1/\kappa)}{\sigma\sqrt{2\pi}}\exp\left\{-\frac{1}{2\sigma^2}[\mathcal{I}(\kappa)+\bar{\mathcal{I}}]^2\right\}, \tag{24b}$$

$$f_{\mathrm{II}}^{\pm}(\kappa;\tau)\equiv\frac{\mathcal{I}_s\kappa\mathcal{K}(\kappa)}{\sigma\sqrt{2\pi}}\exp\left\{-\frac{1}{2\sigma^2}[\mathcal{I}(\kappa)\pm\bar{\mathcal{I}}]^2\right\}. \tag{24c}$$

We have chosen the definitions Eq. (24) to simplify the expressions for the phase-space average $\langle\cdot\rangle$ in terms of the variables κ and τ. To do this, we note that for fixed parameters ϕ_1 and $\delta\omega$, there exists a canonical transformation of

$(p,\theta)\leftrightarrow(H,\tau)$ for which the independent evolution parameter becomes the coordinate θ. Since the transformation is canonical, the Jacobian is unity and we have the following relation between the integration measures:

$$dpd\theta = dHd\tau = \frac{dH}{d\kappa}d\kappa d\tau = 4\phi_1\kappa d\kappa d\tau. \tag{25}$$

Assuming that the average action does not change significantly during one period, i.e., that the conditions (12) are met, we can take the nearly time-independent distribution $f(\kappa;\tau)$ outside the integral over τ. Hence, in subsequent calculations we suppress the dependence of f on τ, and the phase-space average is computed in the small-amplitude limit with the integral expression

$$\langle\mathcal{X}\rangle = \int_1^\infty d\kappa \int_0^{\mathcal{T}} d\tau \left[f_{\mathrm{I}}(\kappa)\frac{\mathcal{X}(\kappa,\tau)}{\mathcal{T}(\kappa)} + f_{\mathrm{III}}(\kappa)\frac{\mathcal{X}(-\kappa,\tau)}{\mathcal{T}(\kappa)} \right] + \int_0^1 d\kappa \int_0^{\mathcal{T}} d\tau \left[f_{\mathrm{II}}^-(\kappa)\frac{\mathcal{X}(\kappa,\tau)}{\mathcal{T}(\kappa)} + f_{\mathrm{II}}^+(\kappa)\frac{\mathcal{X}(-\kappa,\tau)}{\mathcal{T}(\kappa)} \right]. \tag{26}$$

As mentioned earlier, the change in $\bar{\mathcal{I}}$ equals the frequency shift in the small-amplitude limit, $\bar{\mathcal{I}}-\omega_L=\delta\omega$, so that we have the freedom to calculate either Eq. (16) or Eq. (20); to make manifest comparisons to previous work, we choose to evaluate the former. In this case, the first iteration of Eq. (18a) results in the Taylor series approximation of the frequency shift given by

$$\delta\omega \approx \bar{\mathcal{I}} - \omega_L \approx -\frac{\varepsilon(\omega_L,\phi_1)}{\dfrac{\partial}{\partial\omega_L}\varepsilon(\omega_L,\phi_1)}, \tag{27a}$$

$$\text{with } \varepsilon(\omega_L,\phi_1) = 1 + \frac{2}{\phi_1}\langle\cos\theta(\kappa,\tau)\rangle_{\bar{\mathcal{I}}=\omega_L}. \tag{27b}$$

To calculate $\varepsilon(\omega_L,\phi_1)$, we need an expression for $\cos\theta = 2\cos^2(\theta/2)-1$. For slow evolution of the parameters $\phi_1(\tau)$ and $\delta\omega(\tau)$, we use the standard pendulum result,

$$\cos(\theta/2) = \begin{cases} \mathrm{cn}(1/\kappa, \kappa\sqrt{\phi_1}\tau) & \text{if } |\kappa|\geq 1 \\ \mathrm{dn}(\kappa, \sqrt{\phi_1}\tau) & \text{if } |\kappa|<1 \end{cases}, \tag{28}$$

where the functions $\mathrm{cn}(\kappa,x)$ and $\mathrm{dn}(\kappa,x)$ are the Jacobi elliptic functions defined in the usual manner via the inverse of the incomplete elliptic integral of the first kind,

$$\cos\mathcal{Y} \equiv \mathrm{cn}(\kappa,\mathcal{W}) \equiv \frac{1}{\kappa}\sqrt{\kappa^2 - 1 + \mathrm{dn}^2(\kappa,\mathcal{W})},$$

$$\text{where } \mathcal{W}(\kappa,\mathcal{Y}) \equiv \int_0^{\mathcal{Y}} ds \frac{1}{\sqrt{1-\kappa^2\sin^2 s}}.$$

Using the phase-space average Eq. (26), the periods Eq. (23), and the expression Eq. (28), the space average of $\cos\theta$ in the pendulum approximation is given by

$$\langle\cos\theta\rangle = \int_1^\infty d\kappa[f_{\mathrm{I}}(\kappa)+f_{\mathrm{II}}(\kappa)]\int_0^{\mathcal{K}(1/\kappa)} dx \frac{2\mathrm{cn}^2(1/\kappa,x)-1}{\mathcal{K}(1/\kappa)} + \int_0^1 d\kappa[f_{\mathrm{II}}^-(\kappa)+f_{\mathrm{II}}^+(\kappa)]\int_0^{\mathcal{K}(\kappa)} dy \frac{2\mathrm{dn}^2(\kappa,y)-1}{\mathcal{K}(\kappa)},$$

where we have introduced $x\equiv\kappa\sqrt{\phi_1}\tau$ and $y\equiv\sqrt{\phi_1}\tau$. The integrals over x and y can be performed analytically; using the integral tables of Gradshteyn and Ryzhik (Ref. 27, p. 630), the nonlinear dielectric function is given by

$$\varepsilon(\bar{\mathcal{I}},\phi_1) = 1 + \frac{2}{\phi_1}\int_1^\infty d\kappa[f_{\mathrm{I}}(\kappa)+f_{\mathrm{III}}(\kappa)] \times\left[\frac{2\kappa^2\mathcal{E}(1/\kappa)}{\mathcal{K}(1/\kappa)} + 1 - 2\kappa^2\right] + \frac{2}{\phi_1}\int_0^1 d\kappa[f_{\mathrm{II}}^+(\kappa)+f_{\mathrm{II}}^-(\kappa)]\left(\frac{2\mathcal{E}(\kappa)}{\mathcal{K}(\kappa)}-1\right). \tag{29}$$

Expressions similar to those in Eq. (29) were previously derived by Bénisti and Gremillet.[8]

B. The natural frequency in the linear and small-amplitude limits

In the linear limit, $\phi_1\to 0$, and the mean action is that corresponding to the phase velocity of the infinitesimal wave, so that $\bar{\mathcal{I}}\to\omega_L$. From Eq. (27b), the linear limit is characterized by

$$\lim_{\phi_1\to 0}\varepsilon(\omega_L,\phi_1) = 0. \tag{30}$$

For clarity, we relegate the cumbersome calculations used to evaluate Eq. (30) to the Appendix. There, we show that our assumed distribution gives a concrete prescription for the usual resonance pole occurring when the particle velocity matches that of the wave phase velocity. Denoting the Cauchy Principal Value by $\mathcal{P}$, from Eq. (A3) we have

$$\lim_{\phi_1\to 0}\varepsilon(\omega_L,\phi_1) = 1 + \frac{1}{\sigma^2} + \frac{\omega_L/\sigma}{\sigma^2\sqrt{2\pi}}\mathcal{P}\int_{-\infty}^{\infty} du \frac{e^{-u^2/2}}{u-\omega_L/\sigma}. \tag{31}$$

Setting the linear dielectric function Eq. (31) to zero yields the plasma dispersion relation as found by Vlasov,[28] resulting in a purely real natural frequency. Physically, this lack of linear Landau damping arises because we have assumed that the distribution is essentially phase-mixed. As shown by O'Neil,[22] such phase mixing causes linear Landau damping to be a transient effect that itself damps away on the bounce time scale $\sim 1/(\omega_p\sqrt{\phi_1})$. Although the bounce time diverges as $\phi_1\to 0$, we maintain that our analysis and the dispersion relation Eq. (31) apply to finite-amplitude waves after several bounce periods have passed. In this case, the distribution is nearly uniform in canonical angle and Landau damping will be "washed out." The nonlinear fate of such Langmuir waves is generally considered to be a BGK-type mode; as discussed in Refs. 6 and 29, the dispersion relation of small-

amplitude, sinusoidal BGK waves is that of Vlasov, and is identical to Eq. (31) derived here.

For ϕ_1 small but not infinitesimal, we Taylor expand the dielectric function Eq. (29) in the Appendix, yielding

$$\varepsilon(\omega_L,\phi_1)\approx 1.089\sqrt{\phi_1}\left(\frac{\omega_L^2}{\sigma^2}-1\right)\frac{e^{-\omega_L^2/2\sigma^2}}{\sqrt{2\pi}\sigma^3}. \tag{32}$$

A similar expression for the small-amplitude dielectric has been derived by a number of authors, although there are certain discrepancies in the $O(1)$ prefactor. Our coefficient (1.089) is precisely that obtained by Dewar,[7] who calculated the frequency shift assuming a small but finite sinusoidal wave that is adiabatically excited; other calculations in a similar, adiabatic regime have obtained values of 1.41 (Manheimer and Flynn,[30]), 1.76 (Rose and Russell[10]), and 1.60 (Barnes[31]). It should be noted that these differ somewhat from the coefficient of 1.63 calculated by Morales and O'Neil[12] and separately by Dewar[7] for an instantaneously excited wave (i.e., for the initial value problem). To determine the frequency shift, Refs. 10, 12, and 31 use the dielectric function via an expression similar to Eq. (27a); we will see that this yields reasonable results provided that $\phi_1 \lesssim \sigma^2$.

To complete the small-amplitude analysis of the frequency shift (or, equivalently, the change in $\bar{\mathcal{I}}$), we differentiate the linear dispersion relation Eq. (31), obtaining $\partial\varepsilon(\omega_L,\phi_1)/\partial\omega_L$ in the small-amplitude limit. Using Eqs. (18a) and (32), we find that the frequency shift may be expressed for small values of ϕ_1 by

$$\begin{aligned}\delta\omega &\approx -1.089\omega_L\sqrt{\phi_1}\frac{(\omega_L^2-\sigma^2)e^{-\omega_L^2/2\sigma^2}}{(\omega_L^2-1-\sigma^2)\sqrt{2\pi}\sigma}\\ &= -1.089\sqrt{\phi_1}\frac{\omega_L\sigma^2}{\omega_L^2-1-\sigma^2}f''(u)\big|_{u=\omega_L},\end{aligned} \tag{33}$$

with $f(u)$ the initial Maxwellian velocity distribution function $f(u)\equiv\exp(-u^2/2\sigma^2)/(\sigma\sqrt{2\pi})$.

V. COMPARISON TO SELF-CONSISTENT PARTICLE SIMULATIONS

In this section, we compare our theoretical results for the properties of the slowly driven nonlinear Langmuir waves with those obtained from 1D particle simulations. Before discussing these examples, we make a few comments on the numerical methods. In these single-wavelength simulations, we numerically solve the equations of motion for the electrons and the electric field with periodic boundary conditions, driven by a weak, slowly enveloped external force. For each of N electrons over a single wavelength, the jth electron with coordinate $\zeta_j\equiv kz_j$ experiences the combined self-consistent electrostatic force and prescribed drive, giving rise to the following equation of motion:

$$\begin{aligned}\frac{d^2}{d\tau^2}\zeta_j(\tau) &= \frac{1}{N}\sum_{m=1}^{M}\sum_{\ell=1}^{N}\frac{2}{m}\sin[m\zeta_j(\tau)-m\zeta_\ell(\tau)]\\ &\quad+\mathcal{V}(\tau)\cos(\omega_L\tau+\zeta_j)-\mathcal{E}_0(\tau),\end{aligned} \tag{34}$$

where we have expanded the electrostatic potential in M harmonics, each of which involves a sum over the contributions from the N macroparticles. This is a standard technique within the free-electron laser community,[32] although here we have also retained the DC field $\mathcal{E}_0$,[33] to be calculated using the longitudinal component of the Ampère-Maxwell law,

$$\frac{d}{d\tau}\mathcal{E}_0(\tau)=\frac{1}{N}\sum_{\ell=1}^{N}\frac{d}{d\tau}\zeta_\ell(\tau). \tag{35}$$

For the examples shown here, we have used $N\approx 10^6$ simulation particles in the bucket and $M\approx 32$ harmonics. We numerically integrate the system Eqs. (34) and (35) for a given drive potential $\mathcal{V}(\tau)$ using a symplectic operator-splitting scheme that is of global second-order accuracy in time.

To compare the simulation results to our theory, we slowly turn on the ponderomotive drive, ramping the electrostatic field to a chosen amplitude, after which we slowly turn off the drive. By taking the (discrete) Hilbert transform of the potential ϕ, we obtain the total slowly varying frequency $(\omega_L+\delta\omega)$, from which we extract the frequency shift for a given fundamental amplitude ϕ_1. These results are shown in Fig. 4, where we compare the frequency shift $\delta\omega$ extracted from simulations to the following: the shift $\delta\omega_{\mathrm{BG}}$ (dashed line) predicted by the theory of and Bénisti and Gremillet[8] using invariance of J_{BG}, i.e., neglecting $\mathcal{E}_0$, the shift $\delta\omega_{\mathrm{c}}$ (solid line) derived from our theory based on the adiabatic invariance of J_{c}, as well as the lowest-order result (dotted line) given by Dewar,[7] $\delta\omega_{\mathrm{D}}\sim\sqrt{\phi_1}f''(\bar{\mathcal{I}})$, expressed in Eq. (33) (and similar to that in Morales and O'Neil [12]), all for three different values of $k\lambda_D\equiv\sigma$: 0.4 (a), 0.3 (b), and 0.2 (c). We obtain the $\delta\omega_{\mathrm{BG}}$ curve (dashed line), for which it is assumed that J_{BG} is conserved, by solving Eq. (18) and taking $\delta\omega_{\mathrm{BG}}=\bar{\mathcal{I}}-\omega_L$ of the untrapped particles. Our theory uses the mean area $\bar{\mathcal{I}}$ to determine the frequency shift $\delta\omega_{\mathrm{c}}$ via the Ampère-Maxwell law Eq. (20).

The range of ϕ_1 over which $\delta\omega$ was measured in Fig. 4 includes all electrostatic amplitudes that were attained via excitation with the drive amplitude $\mathcal{V}=0.01$ and drive frequency at the linear resonance ω_L. Further driving of the plasma results in a ringing of ϕ_1 that we interpret as resulting from the detuning of the nonlinear Langmuir wave from the external drive (as first observed and explained numerically by Cohen and Kaufman [34]).

As we can see in Fig. 4, the Bénisti and Gremillet theory essentially agrees with our results assuming that $\phi_1\lesssim\sigma^2$, but deviates at larger values of the potential. For warm plasmas such that $\sigma=0.4$, Fig. 4(a) shows that the two theories closely agree over the entire range of attained values of ϕ_1, with the numerical results overlapping the two theoretical predictions within the combined measurement and sampling error of our simulations. In this case, the action $J_{\mathrm{BG}}\approx J_{\mathrm{c}}$ and so is essentially conserved.

For colder plasmas that can be driven to larger amplitudes, however, the discrepancy between the theories becomes apparent. Figure 4(b) indicates that while the qualitative features of the two theories are similar for $\sigma=0.3$, their quantitative predictions can differ by nearly a factor of 2, with the numerical solutions favoring our theory. Finally, assuming J_{BG} is conserved results in an incorrect sign of the

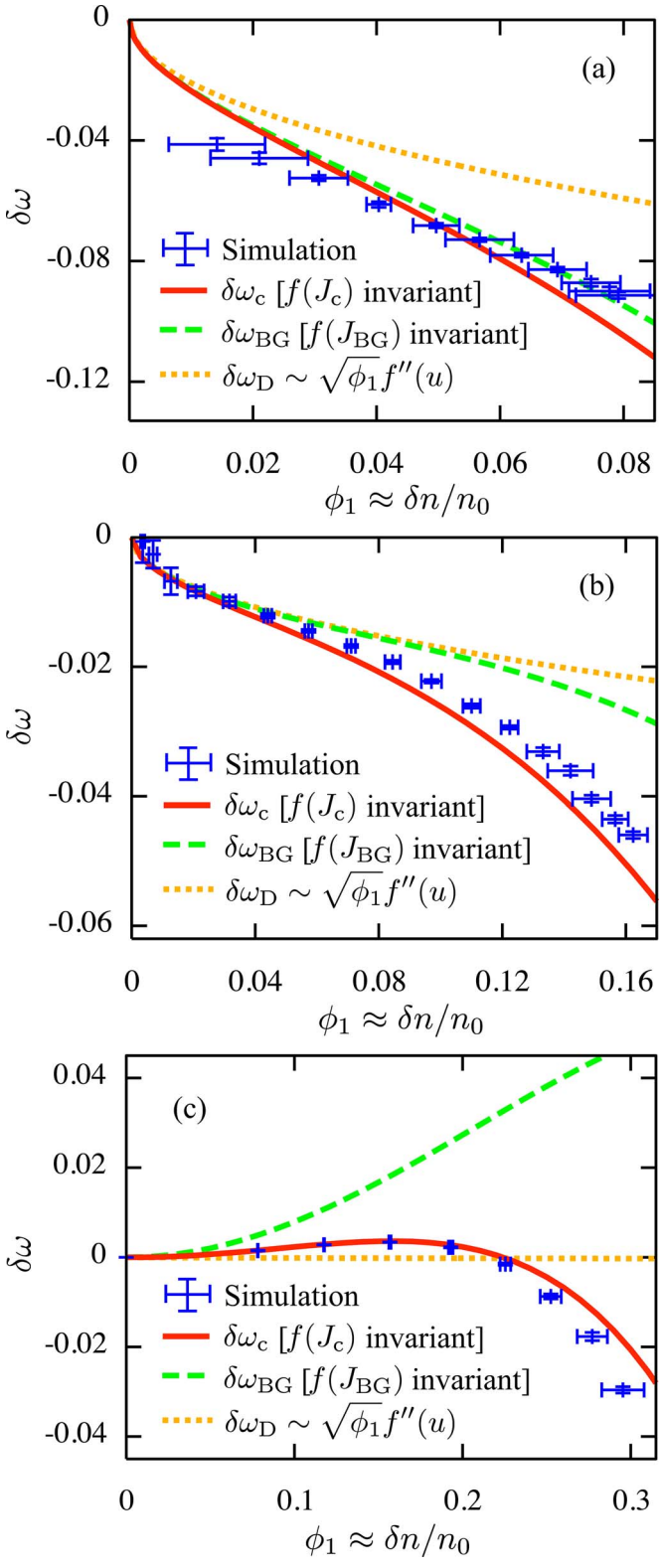

FIG. 4. (Color online) Frequency shift for three different temperatures: $k\lambda_D$=0.4 (a), $k\lambda_D$=0.3 (b), and $k\lambda_D$=0.2 (c). The points are obtained from particle simulations, with error bars indicating two standard deviations in the measured data. We see that the theoretical curve of $\delta\omega_c$ assuming that the distribution in invariant in the canonical action J_c (solid line) agrees quite well with the simulation results, which are closely represented by the theory of constant J_{BG} only for $\phi \lesssim \sigma^2$ (dashed line); we also include the lowest-order approximation $\delta\omega_D \sim f''(v)\sqrt{\phi}$ obtained by Dewar (dotted line), derived here as Eq. (33). To calculate our theoretical frequency shift, we obtain f by solving the iterated equations associated with a distribution invariant in $\mathcal{I}-\bar{\mathcal{I}}(\tau)$, Eq. (18), and use Eq. (20) to obtain $\delta\omega_c$.

frequency shift $\delta\omega_{BG}$ for the relatively cold plasma σ=0.2, while our inclusion of $\mathcal{E}_0$ when calculating the action J_c leads to a shift $\delta\omega_c$ closely following the simulation data. We note that while $\mathcal{E}_0$ always vanishes exactly in the absence of external forcing, and in this case is small even while the forcing is applied, its time integral accumulates and results in a significant correction.

VI. CONCLUSIONS

We have presented a nonlinear longitudinal electron distribution function that naturally arises for slowly driven Langmuir waves, and is parametrized by the amplitude of the electrostatic potential. The distribution function is invariant in the complete canonical action J_c, and the associated frequency shift is determined by the constraints of self-consistency with the slowly growing electrostatic potential. This nonlinear frequency shift agrees well with full particle simulations, and could be used in a reduced, fluid-like model for driven plasmas. Furthermore, the asymptotic distribution function invariant in J_c hints at a simplified model of nonlinear Landau damping via the dynamical process of phase-mixing. Ongoing research aims to use these results as the kinetic foundation of an extended three-wave model of Raman backscatter in a thermal plasma.

ACKNOWLEDGMENTS

The authors would like to acknowledge useful discussions with R. L. Berger and D. J. Strozzi. We are also indebted to D. Bénisti and the anonymous referee for careful reading and commentary.

This work was supported by the University Education Partnership Program through the Lawrence Livermore National Laboratory and by DOE Grant No. DE-FG02-04ER41289.

APPENDIX: LINEAR AND SMALL-AMPLITUDE INTEGRALS FOR $\bar{\mathcal{I}}$, $\delta\omega$

To evaluate the linear and small-amplitude limits of the dielectric function $\varepsilon(\omega_L, \phi_1)$, we first integrate Eq. (29) by parts. The boundary terms at $\kappa=0, \pm\infty$ vanish, while those at $\kappa=1$ cancel, resulting in the following formula for the nonlinear dielectric function:

$$\varepsilon(\omega_L,\phi_1) = 1 + \int_1^\infty d\kappa \frac{h(\kappa)}{\mathcal{I}_s}\{f_I(\kappa)[\mathcal{I}(\kappa)-\omega_L] + f_{III}(\kappa) \times [\mathcal{I}(\kappa)+\omega_L]\} + \int_0^1 d\kappa \frac{q(\kappa)}{\mathcal{I}_s}\{f_{II}^-(\kappa)[\mathcal{I}(\kappa) - \omega_L] + f_{II}^+(\kappa)[\mathcal{I}(\kappa)+\omega_L]\}, \quad \text{(A1)}$$

where

$$h(\kappa) \equiv \frac{32}{3\pi^2\sigma^2}[(2\kappa^3-\kappa)\mathcal{E}(1/\kappa)-2(\kappa^3-\kappa)\mathcal{K}(1/\kappa)],$$

$$q(\kappa) \equiv \frac{32}{3\pi^2\sigma^2}[(2\kappa^2-1)\mathcal{E}(\kappa)-(\kappa^2-1)\mathcal{K}(\kappa)].$$

First, we calculate Eq. (A1) in the linear limit, for which $\phi_1 \to 0$. In this case, the integrals over the trapped electrons (for which $0 \le \kappa \le 1$) make no contribution, while the remaining integrand vanishes exponentially for small κ. Thus, we consistently take $\kappa \gg 1$, for which we have

$$\frac{h(\kappa)}{\mathcal{I}_s} f_1(\kappa) \approx \left[\frac{1}{\kappa}+O\left(\frac{1}{\kappa^3}\right)\right]\frac{e^{-1/2\sigma^2\,[\mathcal{I}(\kappa)-\bar{\mathcal{I}}]^2}}{\sqrt{2\pi}\sigma^3}, \tag{A2a}$$

$$\mathcal{I}(\kappa) \equiv \mathcal{I}_s \kappa \mathcal{E}(1/\kappa) \approx 2\kappa\sqrt{\phi_1}+O(1). \tag{A2b}$$

Defining the integration variables x and y such that

$$\sigma x \equiv 2\kappa\sqrt{\phi_1}+\omega_L, \quad \sigma y \equiv -2\kappa\sqrt{\phi_1}+\omega_L,$$

and using the large κ relations Eq. (A2), we find that the linear relation $\lim_{\phi_1\to 0}\varepsilon(\omega_L,\phi_1)=0$ is given by

$$0 = 1+\frac{1}{\sigma^2}+\frac{\omega_L/\sigma}{\sqrt{2\pi}\sigma^2}\lim_{\delta\to 0}\left\{\int_{\omega_L/\sigma+\delta}^{\infty} dx \frac{e^{-x^2/2}}{x-\omega_L/\sigma} + \int_{-\infty}^{\omega_L/\sigma-\delta} dy \frac{e^{-y^2/2}}{y-\omega_L/\sigma}\right\}, \tag{A3}$$

where $\delta \equiv 2\sqrt{\phi_1}$. As we can see, the assumed distribution function yields a prescription for treating the pole at $x=\omega_L/\sigma$: the symmetric limit is merely the principal value. Note that this is the standard resonance pole occurring when the particle velocity equals the phase velocity of the wave (i.e., when the particle action equals that of the separatrix defined by the infinitesimal wave), and the symmetric limit results in the Vlasov-type dispersion relation Eq. (31). Furthermore, differentiation yields the quantity $\partial\varepsilon(\omega_L,0)/\partial\omega_L$ relevant for the calculation of the change in the frequency (or the change in $\bar{\mathcal{I}}$). Using the dispersion relation Eq. (31), we find

$$\lim_{\phi_1\to 0}\frac{\partial}{\partial\omega_L}\varepsilon(\omega_L,\phi_1) = \frac{1}{\omega_L\sigma^2}(\omega_L^2-1-\sigma^2). \tag{A4}$$

We continue by calculating the change in $\bar{\mathcal{I}}$ [Eq. (27a)] induced by the near-resonant particles, assuming the amplitude of the potential ϕ_1 is small. To make the integrals defining $\varepsilon(\omega_L,\phi_1)$ manifestly convergent, we start by first "rewriting the 1" in the expression for the dielectric Eq. (A1). Assuming the linear dispersion relation Eq. (31) is satisfied, in terms of the energy κ we have

$$1 = -\mathcal{P}\int_{-\infty}^{\infty} d\kappa (2\kappa\sqrt{\phi_1}-\omega_L)\frac{e^{-1/2\sigma^2(2\sqrt{\phi_1}\kappa-\omega_L)^2}}{\kappa\sqrt{2\pi}\sigma^3}. \tag{A5}$$

By appropriate choice of signs for κ, we can express Eq. (A5) as a sum of integrals whose limits are such that $1 \le \kappa < \infty$ or $0 \le \kappa \le 1$, that we then use to replace the leading 1 in the nonlinear dielectric function Eq. (A1). Thus, the nonlinear dielectric is given by

$$\begin{aligned}\varepsilon(\omega_L,\phi_1) = &\int_1^{\infty} d\kappa[\mathcal{I}(\kappa)-\omega_L]h(\kappa)f_{\mathrm{I}}(\kappa)\\ &+\int_1^{\infty} d\kappa[\mathcal{I}(\kappa)+\omega_L]h(\kappa)f_{\mathrm{III}}(\kappa)\\ &+\int_0^{1} d\kappa[\mathcal{I}(\kappa)-\omega_L]q(\kappa)f_{\mathrm{II}}^{-}(\kappa)\\ &+\int_0^{1} d\kappa[\mathcal{I}(\kappa)+\omega_L]q(\kappa)f_{\mathrm{II}}^{+}(\kappa)+1,\end{aligned} \tag{A6}$$

where the pure number 1 is to be interpreted here as the sum of integrals from Eq. (A5). In this manner, the expression Eq. (A6) is perfectly well-defined in the small-amplitude limit, and this limit is simple to calculate numerically. Taylor expanding the integrals with $1 \le \kappa < \infty$, we have

$$\sqrt{\phi_1}\frac{256}{3\pi^2}\int_1^{\infty} d\kappa\left(\frac{3\pi^3}{64}-h(\kappa)\kappa\mathcal{E}(1/\kappa)\mathcal{K}(1/\kappa)\right) \times\left(\frac{\omega_L^2}{\sigma^2}-1\right)\frac{e^{-\omega_L^2/2\sigma^2}}{\sigma\sqrt{2\pi}} \approx -1.50\sqrt{\phi_1}\left(\frac{\omega_L^2}{\sigma^2}-1\right)\frac{e^{-\omega_L^2/2\sigma^2}}{\sqrt{2\pi}\sigma^3},$$

while the last two integrals of Eq. (A6) yield

$$\sqrt{\phi_1}\int_0^1 d\kappa\left\{1-\frac{64\kappa}{3\pi^3}q(\kappa)\mathcal{K}(\kappa)[\mathcal{E}(\kappa)+(\kappa^2-1)\mathcal{K}(\kappa)]\right\} \times 4\left(\frac{\omega_L^2}{\sigma^2}-1\right)\frac{e^{-\omega_L^2/2\sigma^2}}{\sigma\sqrt{2\pi}} \approx 2.59\sqrt{\phi_1}\left(\frac{\omega_L^2}{\sigma^2}-1\right)\frac{e^{-\omega_L^2/2\sigma^2}}{\sqrt{2\pi}\sigma^3}.$$

Adding these contributions, we find that the small-amplitude behavior of the nonlinear dielectric is

$$\lim_{\phi_1\to 0}\varepsilon(\omega_L,\phi_1) = 1.089\sqrt{\phi_1}\left(\frac{\omega_L^2}{\sigma^2}-1\right)\frac{e^{-\omega_L^2/2\sigma^2}}{\sqrt{2\pi}\sigma^3}. \tag{A7}$$

[1] N. G. Van Kampen, Physica (Amsterdam) **21**, 949 (1955).
[2] K. M. Case, Ann. Phys. (N.Y.) **7**, 349 (1959).
[3] L. Landau, J. Phys. (USSR) **10**, 25 (1946).
[4] J. D. Jackson, J. Nucl. Energy, Part C **1**, 171 (1960).
[5] I. B. Bernstein, J. M. Greene, and M. D. Kruskal, Phys. Rev. **108**, 546 (1957).
[6] J. P. Holloway and J. J. Dorning, Phys. Rev. A **44**, 3856 (1991).
[7] R. L. Dewar, Phys. Fluids **15**, 712 (1972).
[8] D. Bénisti and L. Gremillet, Phys. Plasmas **14**, 042304 (2007).
[9] R. L. Berger, C. H. Still, E. A. Williams, and A. B. Langdon, Phys. Plasmas **5**, 4337 (1998).
[10] H. A. Rose and D. A. Russell, Phys. Plasmas **8**, 4784 (2001).
[11] H. X. Vu, D. F. DuBois, and B. Bezzerides, Phys. Plasmas **9**, 1745 (2002).
[12] G. J. Morales and T. M. O'Neil, Phys. Rev. Lett. **28**, 417 (1972).
[13] J. R. Cary, D. F. Escande, and J. L. Tennyson, Phys. Rev. A **34**, 4256 (1986).
[14] A. I. Neishtadt, Sov. J. Plasma Phys. **12**, 568 (1986).
[15] J. H. Hannay, J. Phys. A **19**, L1067 (1986).
[16] R. L. Dewar, Phys. Fluids **16**, 431 (1973).
[17] A. V. Timofeev, Sov. Phys. JETP **48**, 656 (1978).
[18] R. W. B. Best, Physica (Amsterdam) **40**, 182 (1968).
[19] J. R. Cary and R. T. Skodje, Phys. Rev. Lett. **61**, 1795 (1988).
[20] J. R. Cary and R. T. Skodje, Physica D **36**, 287 (1989).
[21] Y. Elskens and D. F. Escande, Nonlinearity **4**, 615 (1991).

[22]T. M. O'Neil, Phys. Fluids **8**, 2255 (1965).
[23]V. I. Arnold, *Mathematical Methods of Classical Mechanics* (Springer-Verlag, New York, 1997).
[24]C. J. McKinstrie and M. Yu, Phys. Fluids B **3**, 3041 (1991).
[25]G. Shvets, N. J. Fisch, and A. Pukhov, IEEE Trans. Plasma Sci. **28**, 1194 (2000).
[26]A. J. Lichtenberg and M. A. Lieberman, *Regular and Stochastic Motion* (Springer-Verlag, New York, 1987).
[27]*Table of Integrals, Series, and Products*, edited by I. S. Gradshteyn and I. M. Ryzhik (Academic, New York, 1980).
[28]A. Vlasov, J. Phys. (USSR) **9**, 25 (1945).
[29]M. Buchanan and J. Dorning, Phys. Rev. E **52**, 3856 (1995).
[30]W. M. Manheimer and R. W. Flynn, Phys. Fluids **14**, 2393 (1971).
[31]D. C. Barnes, Phys. Plasmas **11**, 903 (2004).
[32]W. B. Colson and R. K. Ride, Phys. Lett. **76A**, 379 (1980).
[33]G. Shvets, J. S. Wurtele, and B. A. Shadwick, Phys. Plasmas **4**, 1872 (1997).
[34]B. I. Cohen and A. N. Kaufman, Phys. Fluids **20**, 1113 (1972).